An EM Optimization Method with Adjoint-Sensitivity-Based Multifeature Surrogate for the Design of Microwave Filters

***Abstract*— This paper presents an efficient electromagnetic (*EM*) optimization method with adjoint-sensitivity-based multifeature surrogate for the design of microwave filters. This method is designed to solve the EM optimization problem where the starting point is far from the design specifications. Feature sensitivities are incorporated into the multifeatured surrogate modeling to achieve a surrogate with higher accuracy compared to the existing methods during the EM optimization process. A new design objective function in the feature space is also utilized to improve the speed of multifeature surrogate optimization. A microwave filter example is presented to illustrate this optimization method.**

***Index Terms*— Adjoint feature sensitivity, electromagnetic (*EM*) optimization, microwave filter, surrogate modeling.**

I. Introduction

Direct electromagnetic (EM) optimization is commonly used in the design of microwave filters, which is effective but time-consuming [1]–[5]. To meet the design specifications, several hours or days of repetitive EM simulations may be needed to achieve the optimal solution. To address this problem, EM-driven surrogate-based optimization [6], [7] and its variant with sensitivities are introduced to accelerate the convergence of EM optimization. On the other hand, feature-based EM optimization methods using multifeature surrogate models [8], [9] are also introduced to improve the EM optimization efficiency when the initial design response is far away from the design specification.

In this paper, by taking advantages of the beneficial properties of surrogates with sensitivities and feature-assisted EM optimization, we present an efficient EM optimization method with adjoint-sensitivity-based multifeature surrogate for the design of microwave filters [10]. During the EM optimization process, feature sensitivities are incorporated into the multifeature surrogate modeling. These sensitivities are derived from the EM responses through a six-step extraction approach. In addition, a new design objective function with weighted feature heights of the filter response is also introduced to optimize all feature heights simultaneously, facilitating a quicker convergence towards the design specification.

II. EM Optimization with Multifeature Sensitivities

The EM optimization is an iterative process. In each iteration, multifeature surrogate modeling and multifeature surrogate optimization are performed.

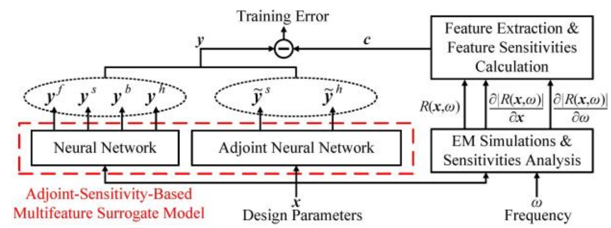

Fig. 1 Structure and training mechanism of the sensitivity-based multifeatured surrogate model [10].

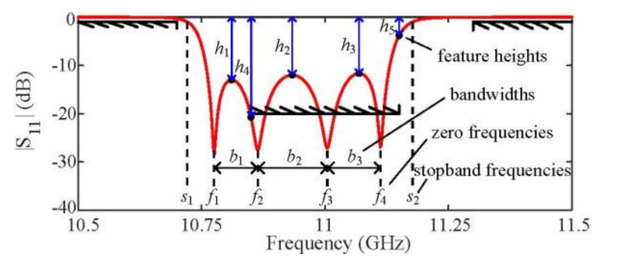

Fig. 2 Presentation of features and sensitivities in the S_{11} response of a fourth-order waveguide filter example at one geometrical sample [10].

A. Multifeature Surrogate Modeling

Fig. 1 shows the structure of sensitivity-based multifeature surrogate model, which consists of one original neural network and its adjoint neural network. Both neural networks share identical inputs and internal weights. The model inputs, denoted as $\boldsymbol{x} = [\, x_1,\ x_2, \dots,\ x_M]^T$, encompass M design parameters in an EM design. The model outputs, denoted as $\boldsymbol{y} = [\boldsymbol{y}^f,\ \boldsymbol{y}^s,\ \boldsymbol{y}^b,\ \boldsymbol{y}^h,\ \tilde{\boldsymbol{y}}^s,\ \tilde{\boldsymbol{y}}^h]^T$, encompass four categories of feature parameters and two feature sensitivity categories.

After EM simulations, we can obtain the EM response and EM sensitivities at different geometrical samples to develop the multifeature surrogate. A six-step extraction approach is presented to extract the zero feature frequencies $\boldsymbol{f}^j$, the stopband feature frequencies $\boldsymbol{s}^j$ and their sensitivities $\tilde{\boldsymbol{s}}^j$, the feature bandwidths $\boldsymbol{b}^j$ and the feature heights $\boldsymbol{h}^j$ as well as their sensitivities $\tilde{\boldsymbol{h}}^j$ to train the sensitivity-based multifeatured surrogate, as shown in Fig. 2.

Step 1: Extract zeros and poles of the transfer function $\boldsymbol{H}^j(\omega)$ from the EM response $R(\boldsymbol{x}^j, \omega)$ by vector fitting. For an N_O-th order filter, we pick N_O effective zeros with relatively small real parts and positive imaginary parts. The corresponding $\boldsymbol{f}^j$ with these zeros are calculated as

$$\boldsymbol{f}^j = \left[f_1^j, f_2^j, \dots, f_i^j, \dots, f_{N_O}^j\right]^T \tag{1}$$

$$f_i^j = \frac{\mathrm{Im}(Z_i^j)}{2\pi}, \quad i = 1,2,\ldots,N_o \tag{2}$$

where Z_i^j represents the ith effective zero obtained from the EM response $R(\boldsymbol{x}^j,\omega)$ of the jth geometrical sample.

Step 2: Extract $\boldsymbol{s}^j$ based on the stopband criteria $|R(\boldsymbol{x}^j,\omega)| \geq h_s$ for $\omega \leq f_{s,1}$ and $\omega \geq f_{s,2}$, where $f_{s,1}$ and $f_{s,2}$ represents the lower and upper frequency boundaries of the stopband respectively, namely,

$$\boldsymbol{s}^j = [s_1^j, s_2^j]^T \tag{3}$$

$$s_1^j = max\left(arg \min_{\omega < f_1^j} |\boldsymbol{H}^j(\omega) - h_s|\right) \tag{4}$$

$$s_2^j = max\left(arg \min_{\omega > f_{N_o}^j} |\boldsymbol{H}^j(\omega) - h_s|\right) \tag{5}$$

Step 3: Extract the sensitivities $\tilde{\boldsymbol{s}}^j$, namely,

$$\tilde{\boldsymbol{s}}^j = \left[\frac{\partial s_1^j}{\partial x_1^j}, \frac{\partial s_1^j}{\partial x_2^j}, \ldots, \frac{\partial s_1^j}{\partial x_m^j}, \ldots, \frac{\partial s_1^j}{\partial x_M^j}, \frac{\partial s_1^j}{\partial x_1^j}, \ldots, \frac{\partial s_1^j}{\partial x_m^j}, \ldots \frac{\partial s_1^j}{\partial x_M^j}\right]^T \tag{6}$$

$$\frac{\partial s_1^j}{\partial x_m^j} = -\left(\frac{\partial |R(\boldsymbol{x}^j,\omega)|}{\partial \omega}\right)^{-1} \cdot \left.\frac{\partial |R(\boldsymbol{x}^j,\omega)|}{\partial x_m^j}\right|_{\omega = s_1^j} \tag{7}$$

$$\frac{\partial s_2^j}{\partial x_m^j} = -\left(\frac{\partial |R(\boldsymbol{x}^j,\omega)|}{\partial \omega}\right)^{-1} \cdot \left.\frac{\partial |R(\boldsymbol{x}^j,\omega)|}{\partial x_m^j}\right|_{\omega = s_2^j} \tag{8}$$

Step 4: Extract $\boldsymbol{b}^j$ using $\boldsymbol{f}^j$, namely,

$$\boldsymbol{b}^j = [b_1^j, b_2^j, \ldots, b_i^j, \ldots, b_{N_o-1}^j]^T \tag{9}$$

$$b_i^j = f_{i+1}^j - f_i^j, \quad i = 1, 2, \ldots, N_o - 1 \tag{10}$$

Step 5: Extract $\boldsymbol{h}^j$, which encompasses $N_o - 1$ ripples and two passband boundaries, adhering to the passband criteria $|R(\boldsymbol{x}^j,\omega)| \leq h_p$, $f_{p,1} \leq \omega \leq f_{p,2}$. Here, h_p represents the passband response specification, while $f_{p,1}$ and $f_{p,2}$ denote the lower and upper frequency boundaries of the passband, respectively. The ripples are determined as the maximum values of $H^j(\omega)$ between two adjacent zero feature frequencies. To emphasize the variation around the passband response specification, a nonlinear transformation is applied to the values of $H^j(\omega)$, namely,

$$\boldsymbol{h}^j = [h_1^j, h_2^j, \ldots, h_i^j, \ldots, h_{N_o+1}^j]^T \tag{11}$$

$$h_i^j = \frac{2}{1 + e^{\lambda\left(H^j\left(f_{h,i}^j\right) - h_p\right)}}, \quad i = 1, 2, \ldots, N_o + 1 \tag{12}$$

$$f_{h,i}^j = arg \max_{f_i^j \leq \omega \leq f_{i+1}^j} |H^j(\omega)|, \quad i = 1, 2, \ldots, N_o - 1 \tag{13}$$

$$f_{h,N_o}^j = f_{p,1}, \qquad f_{h,N_o+1}^j = f_{p,2} \tag{14}$$

where h_i^j represents the transformed ith feature height, λ is the transformation coefficient for $H^j(\omega)$, and $f_{h,i}^j$ is the frequency corresponding to the ith feature height.

Step 6: Extract the sensitivities $\tilde{\boldsymbol{h}}^j$, namely,

$$\tilde{\boldsymbol{h}}^j = \left[\frac{\partial h_1^j}{\partial x_1^j}, \frac{\partial h_1^j}{\partial x_2^j}, \ldots, \frac{\partial h_i^j}{\partial x_m^j}, \ldots \frac{\partial h_{N_o+1}^j}{\partial x_M^j}\right]^T \tag{15}$$

$$\frac{\partial h_i^j}{\partial x_m^j} = \frac{-2\lambda e^{\lambda\left(h_i^j - h_p\right)}}{\left(e^{\lambda\left(h_i^j - h_p\right)} + 1\right)^2} \frac{\partial \left|R\left(x^j, f_{h,i}^j\right)\right|}{\partial x_m^j},$$
$$i = 1, 2, \ldots, N_o + 1 \tag{16}$$

We use the vector $\boldsymbol{c}^j$ to indicate the target output of the model corresponding to the jth geometrical sample, i.e.,

$$\boldsymbol{c}^j = \left[(\boldsymbol{f}^j)^T, (\boldsymbol{s}^j)^T, (\boldsymbol{b}^j)^T, (\boldsymbol{h}^j)^T, (\tilde{\boldsymbol{s}}^j)^T, (\tilde{\boldsymbol{h}}^j)^T\right]^T \tag{17}$$

To train the desired adjoint-sensitivity-based multifeature surrogate, the above steps are applied to all geometric samples to obtain training data.

B. Multifeature Surrogate Optimization

After developing the multifeatured surrogate, EM optimization using the developed multifeature surrogate requires a comprehensive objective function within the feature space, i.e.,

$$U(x) = U_f + U_s + U_b + U_h \tag{18}$$

where U_f, U_s and U_b represent the least square errors corresponding to design specifications and $\boldsymbol{y}^f$, $\boldsymbol{y}^s$, and $\boldsymbol{y}^b$, respectively. For U_h, proportional weights T_i are added in $\boldsymbol{y}^h$, i.e.,

$$T_i = 1 + \frac{1 - y_i^h}{1 - min\{y_1^h, y_2^h, \ldots, y_i^h, \ldots, y_{N_o-1}^h\}} \tag{19}$$

$$U_h^+ = \begin{cases} \sum_{i=1}^{N_o-1} [T_i(\max\{1 - y_i^h, 0\})^2], & U_s > 0 \\ \sum_{i=1}^{N_o+1} [T_i(\max\{1 - y_i^h, 0\})^2], & \text{else} \end{cases} \tag{20}$$

$$U_h^- = -\sum_{i=1}^{N_o+1} (y_i^h - 1)^{-2} \tag{21}$$

$$U_h = \begin{cases} U_h^+, & U_f + U_s + U_b + U_h^+ > 0 \\ U_h^-, & \text{else} \end{cases} \tag{22}$$

where y_i^h denotes the ith feature height. Incorporating T_i in (22) facilitates the alignment of feature heights to the greatest extent possible during the optimization process, hastening the approach towards meeting the design specifications.

The EM optimization proceeds iteratively until

$$\left\|\frac{U\left(x^{(k)}\right) - U\left(x^{(k-1)}\right)}{U\left(x^{(k-1)}\right)}\right\| \leq \varepsilon \tag{23}$$

is achieved, as shown in Fig. 3.

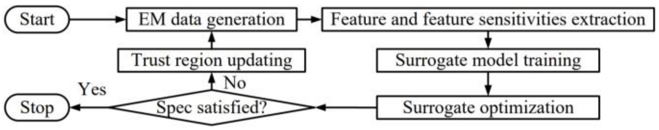

Fig. 3 Flowchart of the presented EM optimization [10].

III. Application Example

In this example, we apply the EM optimization method to design an iris coupled cavity filter[11], [12] as shown in Fig. 4(a). The optimization results using different methods are shown in Tables I and Fig. 4(b). The design parameters are $\boldsymbol{x} = [H_{c1}, H_{c2}, H_{c3}, W_1, W_2, W_3, W_4]^T$ and the effective order of the filter is 6. The design specifications are $|S_{11}| \leq -20$ dB in 703-713MHz and $|S_{11}| \geq -1$ dB in 690-701MHz and 715-720MHz. Two starting points are $\boldsymbol{x}_1 = [46.7, 53.8, 54.2, 119.0, 53.9, 48.2, 48.4]^T$ and $\boldsymbol{x}_2 = [38.8, 45.9, 45.5, 111.8, 46.1, 44.0, 45.1]^T$ (mm), respectively.

According to the filter optimization steps, we first obtain the EM response of each sample through EM simulation. The features and their sensitivity information are then extracted by (1)-(16), and the extracted data are used to train the adjoint-sensitivity-based multifeature surrogate. In the end, through the comprehensive objective function, the trained surrogate model iteratively undergoes optimization, exploring optimal solutions and ultimately yielding results that meet the design specifications. Additionally, we employ direct EM optimization method and existing optimization method [9] for comparison.

As shown in Table I and Fig. 4(b), the presented EM optimization method accomplishes the final solution with fewer iterations. For the starting point $\boldsymbol{x}_1$, the presented method takes a total of 4.72 hours, which is 18.76% less than the existing method [9] and 96.52% less than the direct EM method. For the starting point $\boldsymbol{x}_2$, the presented method takes a total of 5.25 hours, reducing by 25.63% and 96.7% respectively. The time consumption for different starting points has been reduced, thus enhancing the efficiency of EM optimization.

IV. Conclusion

This paper presents an efficient EM optimization method with adjoint-sensitivity-based multifeature surrogate model. Multifeature sensitivity information and a new weight objective function is incorporated during EM optimization, effectively improving the EM optimization efficiency.

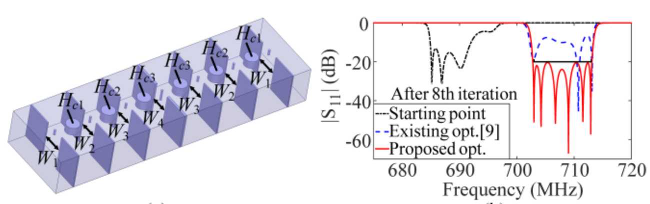

(a) (b)

Fig. 4 (a) Structure and (b) responses of iris coupled cavity filter [10].

TABLE I

Comparison of Results Using Different Methods [10]

Starting point	Methods	Direct EM opt.	Existing opt. [9]	Proposed opt.
$\boldsymbol{x}_1$	No. of iterations	350	13	8
	Simulation time	23.3 min	24.9 min	31.2 min
	Surrogate training time	/	1s×13	19s×8
	Final objective function value	0.11	-68.67	-428.60
	Max stop band $\lvert S_{11}\rvert$	-18.55dB	-20.29dB	-20.21dB
	Total time	135.92h	5.81h	4.72h
$\boldsymbol{x}_2$	No. of iterations	410	16	9
	Final objective function value	1.98	-125.91	-435.62
	Max stop band $\lvert S_{11}\rvert$	-17.67dB	-20dB	-20.05dB
	Total time	159.22h	7.06h	5.25h

References

[1] Z. Zhang, Q. S. Cheng, H. Chen, and F. Jiang, "An Efficient Hybrid Sampling Method for Neural Network-Based Microwave Component Modeling and Optimization," *IEEE Microw. Wirel. Compon. Lett.*, vol. 30, no. 7, pp. 625–628, Jul. 2020.

[2] X. Luo, B. Yang, and H. J. Qian, "Adaptive Synthesis for Resonator-Coupled Filters Based on Particle Swarm Optimization," *IEEE Trans. Microw. Theory Tech.*, vol. 67, no. 2, pp. 712–725, Feb. 2019.

[3] N. Leszczynska, A. Lamecki, and M. Mrozowski, "Fast Full-Wave Multilevel Zero-Pole Optimization of Microwave Filters," *IEEE Microw. Wirel. Compon. Lett.*, vol. 26, no. 11, pp. 867–869, Nov. 2016.

[4] P. Korbel, S. Hausman, and P. Di Barba, "Application of Evolutionary Approach for Multi-objective Improvement of Indoor Access Point Placement," in *2019 13th European Conference on Antennas and Propagation (EuCAP)*, Mar. 2019, pp. 1–4. Accessed: Dec. 23, 2023.

[5] M. O. Akinsolu, B. Liu, V. Grout, P. I. Lazaridis, M. E. Mognaschi, and P. D. Barba, "A Parallel Surrogate Model Assisted Evolutionary Algorithm for Electromagnetic Design Optimization," *IEEE Trans. Emerg. Top. Comput. Intell.*, vol. 3, no. 2, pp. 93–105, Apr. 2019.

[6] Y. Yu, Z. Zhang, Q. S. Cheng, B. Liu, Y. Wang, C. Guo, Terry Tao Ye, "State-of-the-Art: AI-Assisted Surrogate Modeling and Optimization for Microwave Filters," *IEEE Trans. Microw. Theory Tech.*, vol. 70, no. 11, pp. 4635–4651, Nov. 2022.

[7] P. Zhao and K. Wu, "Homotopy Optimization of Microwave and Millimeter-Wave Filters Based on Neural Network Model," *IEEE Trans. Microw. Theory Tech.*, vol. 68, no. 4, pp. 1390–1400, Apr. 2020.

[8] F. Feng, W. Na, W. Liu, S. Yan, L. Zhu, J. Ma, Q.-J. Zhang, "Multifeature-Assisted Neuro-transfer Function Surrogate-Based EM Optimization Exploiting Trust-Region Algorithms for Microwave Filter Design," *IEEE Trans. Microw. Theory Tech.*, vol. 68, no. 2, pp. 531–542, Feb. 2020.

[9] Jing Jin, F. Feng, W. Na, J. Zhang, W. Zhang, Z. Zhao, Q.-J. Zhang, "Advanced cognition-driven EM optimization incorporating transfer function-based feature surrogate for microwave filters," *IEEE Trans. Microw. Theory Tech.*, vol. 69, no. 1, pp. 15–28, Jan. 2021.

[10] W. Na, K. Liu and, W. Zhang, F. Feng, J. Zhang, H. Xie, D. Jin, Q.-J. Zhang, "Advanced EM Optimization Using Adjoint-Sensitivity-Based Multifeature Surrogate for Microwave Filter Design," *IEEE Microw. Wirel. Technol. Lett.*, pp. 1–4, 2023.

[11] F. Feng, C. Zhang, W. Na, J. Zhang, W. Zhang, and Q.-J. Zhang, "Adaptive Feature Zero Assisted Surrogate-Based EM Optimization for Microwave Filter Design," *IEEE Microw. Wirel. Compon. Lett.*, vol. 29, no. 1, pp. 2–4, Jan. 2019.

[12] Y. Cao, S. Reitzinger, and Q.-J. Zhang, "Simple and Efficient High-Dimensional Parametric Modeling for Microwave Cavity Filters Using Modular Neural Network," *IEEE Microw. Wirel. Compon. Lett.*, vol. 21, no. 5, pp. 258–260, May 2011.